Radiology: Cardiothoracic Imaging

CASE SERIES

Cardiac MRI and Clinical Outcomes in *TMEM43* Arrhythmogenic Cardiomyopathy

João Matos, MD • Emmi Helle, MD, PhD • Melanie Care, MSc • Yasbanoo Moayedi, MD, MHSc • Michael H. Gollob, MD • Paaladinesh Thavendiranathan, MD, SM • Danna Spears, MD • Kate Hanneman, MD, MPH

From the Department of Medical Imaging (J.M., P.T., K.H.) and Division of Cardiology (E.H., M.C., Y.M., M.H.G., P.T., D.S.), Peter Munk Cardiac Centre, Toronto General Hospital, University Health Network (UHN), University of Toronto, 585 University Ave, 1 PMB-298, Toronto, ON, Canada M5G 2N2; Department of Paediatrics, Labatt Family Heart Centre, The Hospital for Sick Children, University of Toronto, Toronto, Canada (E.H.); Stem Cells and Metabolism Research Program, Faculty of Medicine, University of Helsinki, Helsinki, Finland (E.H.); Department of Molecular Genetics, University of Toronto, Toronto, Canada (M.C.); and Toronto General Hospital Research Institute, University Health Network (UHN), University of Toronto, Toronto, Canada (M.H.G., P.T., K.H.). Received June 9, 2023; revision requested July 18; revision received October 27; accepted November 9. **Address correspondence to** K.H. (email: *kate.hanneman@uhn.ca*).

Authors declared no funding for this work.

Conflicts of interest are listed at the end of this article.

Radiology: Cardiothoracic Imaging 2023; 5(6):e230155 • https://doi.org/10.1148/ryct.230155 • Content codes: CA MR

Arrhythmogenic cardiomyopathy is an inherited cardiomyopathy that can involve both ventricles. Several genes have been identified as pathogenic in arrhythmogenic cardiomyopathy, including *TMEM43*. However, there are limited data on cardiac MRI findings in patients with *TMEM43* variants to date. In this case series, cardiac MRI findings and clinical outcomes are described in 14 patients with *TMEM43* variants, including eight (57%) with the pathogenic p.Ser358Leu variant (six female patients; mean age, 33 years ± 15 [SD]) and six (43%) with a *TMEM43* variant of unknown significance (three female patients; mean age, 38 years ± 11). MRI findings demonstrated left ventricular systolic dysfunction in eight (57%) patients and right ventricular dysfunction in four (29%) patients. Among the nine patients with late gadolinium enhancement imaging, left ventricular late gadolinium enhancement was present in seven (78%; all subepicardial) patients. In summary, *TMEM43* variants are associated with high prevalence of subepicardial late gadolinium enhancement and left ventricular dysfunction.

Supplemental material is available for this article.

Arrhythmogenic cardiomyopathy (ACM) is an inherited cardiomyopathy that can lead to ventricular arrhythmia and sudden cardiac death (1). ACM was initially described as a disease predominantly involving the right ventricle (2), hence the term *arrhythmogenic right ventricular cardiomyopathy* (ARVC). However, cardiac imaging and histopathologic findings have demonstrated that myocardial fibrofatty replacement can involve both ventricles (3).

ACM usually has autosomal dominant transmission with variable expression. Genes encoding for desmosomal proteins account for approximately half of identified patients with gene-positive ACM (4). Other nondesmosomal genes have also been identified as pathogenic in ACM, including the *TMEM43* gene encoding transmembrane protein 43. The most frequent *TMEM43* variant is a missense variant (*TMEM43* c.1073C>T, p.Ser358Leu), which is fully penetrant and was initially reported as a cause of ARVC type 5 in Newfoundland, Canada, but has since been identified elsewhere (5–7). Despite the often severe phenotypic manifestation, there are limited data on cardiac MRI findings in patients with *TMEM43* variants to date (8,9). The purpose of this case series was to describe cardiac MRI findings and clinical outcomes in patients with *TMEM43* variants, including those with both pathogenic variants (PV) and variants of unknown significance (VUS), while highlighting differences between male and female patients and progression of imaging findings among patients with follow-up imaging.

Description and Analysis

Patients

This retrospective case series was approved by the institutional ethics committee, and the requirement for written informed consent was waived. Consecutive adult (≥18 years of age) patients with a PV or VUS in the *TMEM43* gene who were referred to our tertiary hospital network and had at least one cardiac MRI performed between October 2013 and December 2022 were identified.

All genetic testing was performed at an accredited clinical laboratory, and variants were classified according to 2015 American College of Medical Genetics variant interpretation guidelines (10). Patients were evaluated with respect to ACM using the 2020 Padua criteria (3). Those with left ventricular late gadolinium enhancement (LGE) on MR images and no morphologic, functional, or structural right ventricular criteria were classified as left dominant. Patients who met morphologic, functional, or structural criteria for both left and right ventricles were classified as biventricular. Finally, those who met right ventricular morphologic, functional, or structural criteria and were without left ventricular morphologic, functional, or structural criteria were classified as right dominant. We also evaluated patients using the 2010 modified Task Force criteria for ARVC for comparison (11).

Abbreviations

ACM = arrhythmogenic cardiomyopathy, ARVC = arrhythmogenic right ventricular cardiomyopathy, LGE = late gadolinium enhancement, PV = pathogenic variant, VUS = variant of unknown significance

Summary

Variants in the *TMEM43* gene were associated with high prevalence of subepicardial late gadolinium enhancement and left ventricular dysfunction on cardiac MR images.

Keywords

Arrhythmogenic Cardiomyopathy, Arrhythmogenic Right Ventricular Cardiomyopathy, *TMEM43*, Cardiac MRI, Genetic Variants

Cardiac MRI

Cardiac MRI studies had been performed using 1.5- or 3-T scanners (MAGNETOM Avanto Fit and SKYRA Fit; Siemens Healthineers), including acquisition of long-axis and a stack of short-axis balanced cine steady-state free precession sections (section thickness, 8 mm; intersection gap, 2 mm). Depending on the protocol, LGE images were acquired in some patients using a two-dimensional phase-sensitive inversion-recovery technique starting 12 minutes after administration of intravenous contrast material (0.1–0.2 mmol/kg body weight of gadobutrol; Bayer Healthcare). In patients with MRI performed in 2018 or later, a single midventricular short-axis T1 and T2 mapping section was acquired using a modified Look-Locker inversion-recovery technique for native T1 mapping (5[3]3 inversion grouping), and a matching T2 map was acquired using a T2-prep technique with readout varying with external field strength (fast low-angle shot at 3 T).

Ventricular volumes, function, and mass were measured according to current standards (12). Left and right ventricular dilatation were defined using sex-specific cut points (13). Left and right ventricular systolic dysfunction were defined as a left ventricular ejection fraction less than 55% and a right ventricular ejection fraction less than 50%, respectively. Presence of LGE was evaluated visually (present or not) both globally and according to the American Heart Association 17-segment model (14), and the predominant pattern was classified as subendocardial, midwall, subepicardial, or transmural. A ringlike pattern of LGE was defined as involvement of at least three contiguous segments in the same short-axis section (15). Abnormal maximum T1 and T2 values were defined as 2 SDs above the mean of sequence-specific local reference values (high T2 defined as >45 msec and high T1 defined as >1289 msec at 3 T) (16). In the subset of patients with more than one MRI acquisition, the most remote and most recent MR images were analyzed to evaluate for changes in quantitative parameters over time.

Case Series Findings

Fourteen patients with variants in *TMEM43* were identified (mean age, 35 years ± 13 [SD], nine [64%] female patients, five [36%] male patients; Table S1). Eight patients (57%) carried the pathogenic p.Ser358Leu variant (six [75%] of these patients were female; mean age, 33 years ± 15), and six (43%) patients had a *TMEM43* VUS (three [50%] were female; mean age, 38 years ± 11) (Table 1). None of the patients had an additional variant associated with ACM (including *DSP*) or other cardiomyopathy.

Seven (50%) patients met criteria for biventricular ACM (PV, three; VUS, four) and four (29%) patients met criteria for left-dominant ACM (PV, two; VUS, two). Three (21%) patients did not meet criteria for ACM (all were female patients, had PVs identified through family cascade screening, and were younger than 30 years of age). Only four patients met 2010 modified Task Force criteria for ARVC (all with biventricular ACM; PV, two; VUS, two).

Clinical and Electrocardiographic Findings

Overall, nine of the 14 (64%) patients had at least one cardiac symptom (PV, four; VUS, five), including palpitations in seven patients, chest pain in two patients, and shortness of breath in two patients. High-sensitivity cardiac troponin values were elevated (>26 pg/mL) in two of eight (25%) patients with available values (range, 64–196 pg/mL). B-type natriuretic peptide values were elevated (>100 pg/mL) in two of six (33%) patients with available values (range, 215–504 pg/mL). Five (35%) patients had at least one abnormality at electrocardiography (PV, three; VUS, two) which included a depolarization abnormality in all five patients, repolarization abnormality in three patients, and right bundle branch block in two patients.

Cardiac MRI

Cardiac MRI characteristics are summarized in Table 2. At least one left ventricular abnormality was identified in 11 of 14 (79%) patients, and at least one right ventricular abnormality was identified in eight (57%) patients. All patients with a right ventricular abnormality also had a left ventricular abnormality.

Abnormal left ventricular findings on MR images included left ventricular dilatation in five of 14 (36%; PV, one; VUS, four) patients, right ventricular dilatation in five (36%; PV, three; VUS two) patients, systolic left ventricular dysfunction in eight (57%; PV, four; VUS, four) patients, systolic right ventricular dysfunction in four (29%; PV, two; VUS, two) patients, LGE in seven of nine (78%; PV, four; VUS, three; all subepicardial) patients with LGE imaging, high T1 in three of four (75%; PV, three) patients with mapping, and high T2 in one of four (25%; PV, one) patients with mapping (Figs 1–4, Movie). The most frequent segment with LGE in the nine patients with LGE imaging was the basal inferolateral wall (56%; PV, two; VUS, three), followed by the mid inferolateral wall (44%; PV, three; VUS, one) (Fig 5). Four (44%; PV, three; VUS, one) patients had a ringlike pattern of LGE.

Abnormal right ventricular findings included right ventricular dilatation in five of 14 (36%; PV, three; VUS, two) patients, systolic right ventricular dysfunction in four (29%; PV, two; VUS, two) patients, and right ventricular LGE in four of nine (44%; PV, one; VUS, three) patients with LGE imaging.

Five patients had more than one cardiac MRI acquisition, with a median interval of 6.5 years [IQR, 1.6–9.6]. Two of these five (40%) patients developed new left and right

Table 1: Summary of Patient Characteristics by *TMEM43* Variant Type

Characteristic	All Patients (*n* = 14)	PV (p.Ser358Leu) (*n* = 8)	VUS (*n* = 6)
Age (y)	35 ± 13	33 ± 15	38 ± 11
Sex			
Female	9 (64)	6 (75)	3 (50)
Male	5 (36)	2 (25)	3 (50)
BSA (m^2)	1.8 ± 0.2	1.8 ± 0.1	1.9 ± 0.2
Family history of ACM	8 (57)	8 (100)	0 (0)
Family history of SCD	6 (43)	6 (75)	0 (0)
ACM (Padua criteria)	11 (79)	5 (63)	6 (100)
Biventricular phenotype	7 (50)	3 (38)	4 (67)
Left-dominant phenotype	4 (29)	2 (25)	2 (33)
Any cardiac symptoms	9 (64)	4 (50)	5 (83)
Palpitations	7 (50)	3 (38)	4 (67)
Chest pain	2 (14)	1 (13)	1 (17)
Shortness of breath	2 (14)	1 (13)	1 (17)
Syncope	1 (7)	0 (0)	1 (17)
ECG findings			
ST segment changes	2 (14)	0 (0)	2 (33)
RBBB	2 (14)	1 (13)	1 (17)
LBBB	1 (7)	1 (13)	0 (0)
Depolarization abnormality	5 (36)	3 (38)	2 (33)
Repolarization abnormality	3 (21)	2 (25)	1 (17)

Note.—Variables are presented as means ± SDs or numbers with percentages in parentheses. ACM = arrhythmogenic cardiomyopathy, BSA = body surface area, ECG = electrocardiography, LBBB = left bundle branch block, PV = pathogenic variant, RBBB = right bundle branch block, SCD = sudden cardiac death, VUS = variant of unknown significance.

Table 2: Summary of Cardiac MRI Findings by *TMEM43* Variant Type

Parameter	All Patients (*n* = 14)	PV (*n* = 8)	VUS (*n* = 6)
Left ventricle			
At least one left ventricular abnormality	11 (79)	5 (63)	6 (100)
Dilatation	5 (36)	1 (13)	4 (67)
Systolic dysfunction	8 (57)	4 (50)	4 (67)
Regional wall motion abnormality	8 (57)	3 (38)	5 (83)
LGE presence*	7 (78)	4 (100)	3 (60)
LGE, no. of segments*	3 (1–5)	5 (4–5)	1 (0–2)
High T2†	1 (25)	1 (33)	0 (0)
High native T1†	3 (75)	3 (100)	0 (0)
Right ventricle			
At least one right ventricular abnormality	8 (57)	4 (50)	4 (67)
Dilatation	5 (36)	3 (38)	2 (33)
Systolic dysfunction	4 (29)	2 (25)	2 (33)
Regional wall motion abnormality	6 (43)	3 (38)	3 (50)
LGE presence†	4 (44)	1 (25)	3 (60)

Note.—Variables are presented as numbers with percentages in parentheses or medians with IQRs in parentheses. LGE = late gadolinium enhancement, PV = pathogenic variant, VUS = variant of unknown significance.
* LGE imaging available in nine patients (four patients with PV and five with VUS).
† Mapping available in four patients (three patients with PV and one with VUS).

ventricular abnormalities between baseline and follow-up MRI. Indexed left ventricular end-diastolic volume increased (median, 89 mL/m^2 [IQR, 81–94] vs 101 mL/m^2 [IQR, 83–105]) and left ventricular ejection fraction decreased in the interval (median, 64% [IQR, 62%–64%] vs 56% [IQR, 54%–60%]) in the subset of patients with more than one cardiac MRI acquisition.

Other Cardiac Imaging Findings

Cardiac CT was performed in two (VUS, two) patients, demonstrating macroscopic fat along the left ventricular lateral wall corresponding to areas of subepicardial LGE on MR images in both patients (Figs 1, 2). Thirteen of the (92%; PV, seven; VUS, six) 14 patients underwent transthoracic echocardiography within 1 year of MRI. At echocardiography, left ventricular abnormalities were identified in six (46%; PV, two; VUS, four) patients, and right ventricular abnormalities were identified in two (15%; PV, one; VUS, one) patients.

Sex Differences

Most of the clinical and cardiac MRI findings were similar between male and female patients (Table S2). However, right ventricular dilatation was more frequent in male patients compared with female (four of five [80%] vs one of nine [11%]) patients. Male patients were also more likely to be symptomatic (five of five [100%] vs four of nine [44%]) and to have significant premature ventricular contractions (five of five [100%] vs three of nine [33%]).

Clinical Outcomes

Clinical follow-up was available in all patients included in the case series, with median clinical follow-up duration of 5.4 [IQR, 2.4–6.5] years after MRI. Four of the 14 (29%) patients experienced a major adverse cardiac event (PV, two; VUS, two; median age at first event, 42 [IQR 27–55] years). Nonmutually exclusive events were aborted sudden cardiac death in two (14%) patients, appropriate implanted cardioverter defibrillator discharge in one (7%) patient, and sustained ventricular tachycardia in two (14%) patients. There were no deaths. Nonsustained ventricular tachycardia occurred in eight (57%; PV, five; VUS, three; median age at first event, 40 [IQR 27–54] years) patients and significant premature ventricular beats in eight (57%;

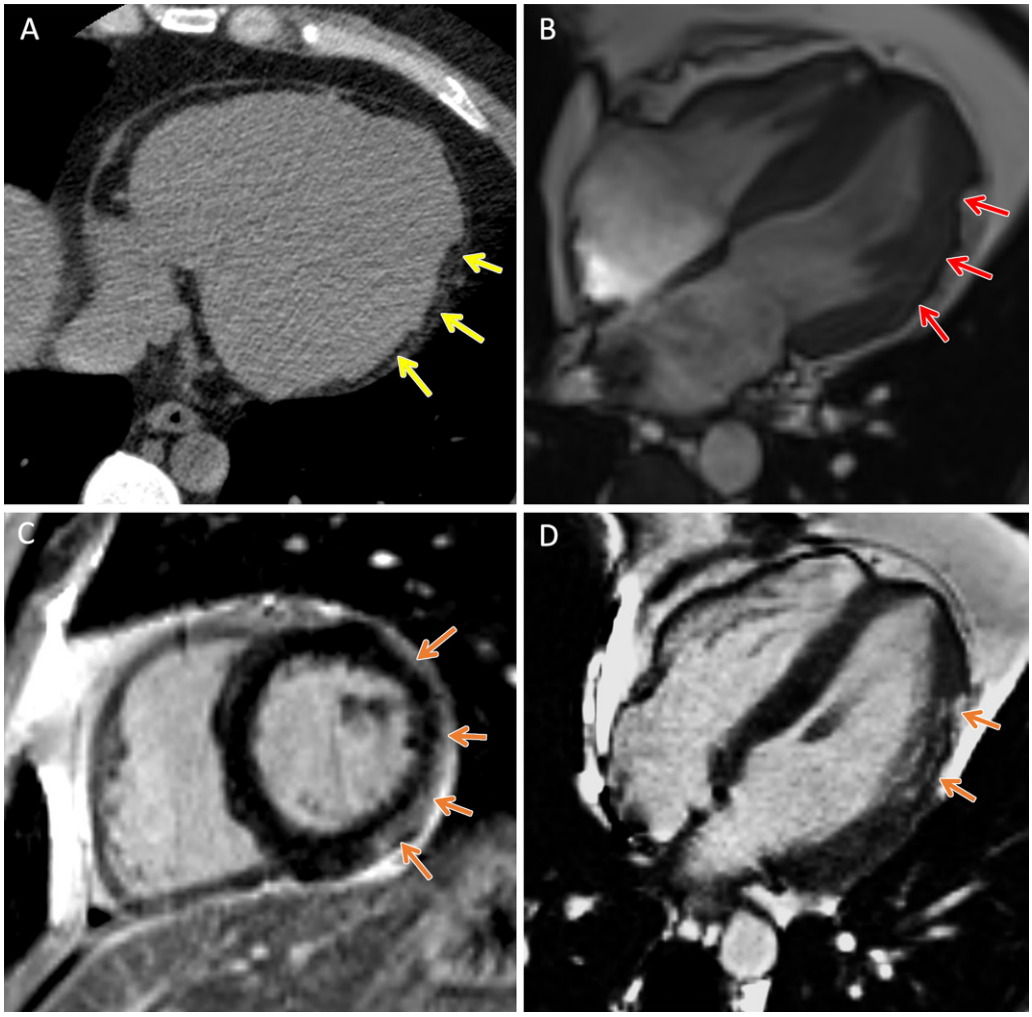

Figure 1: *TMEM43* arrhythmogenic cardiomyopathy. Cardiac CT and MR images in a male patient between 30 and 39 years of age (exact age not provided due to potential reidentification risk) with a *TMEM43* variant of unknown significance (p.Gly280Glu) with palpitations and premature ventricular beats at Holter monitoring. **(A)** Axial noncontrast cardiac CT image demonstrates extensive subepicardial fat along the lateral left ventricular wall (yellow arrows). **(B)** Four-chamber 1.5-T steady-state free precession MR image demonstrates subepicardial chemical shift artifact along the lateral left ventricular wall (red arrows). **(C)** Short-axis and **(D)** four-chamber late gadolinium enhancement images demonstrate subepicardial late gadolinium enhancement involving the midventricular anterolateral wall, inferolateral wall, and inferior wall (orange arrows).

PV, four; VUS, four; median age first event, 33 [IQR, 26–52] years) patients. Among patients with LGE imaging, all of the patients who experienced a major adverse cardiac event and nonsustained ventricular tachycardia had LGE on MR images. None of the patients without LGE experienced a major adverse cardiac event or nonsustained ventricular tachycardia.

Discussion

Although cardiac MRI plays a key role in the diagnosis of ACM, there are currently limited imaging descriptions in patients with *TMEM43* variants to date. In this case series of 14 patients with *TMEM43* variants (eight with the pathogenic p.Ser358Leu variant and six with a *TMEM43* VUS), cardiac MRI demonstrated left ventricular dysfunction in 57%, right ventricular dysfunction in 29%, and subepicardial LGE in 78%. Left ventricular dysfunction was progressive with interval reduction in left ventricular ejection fraction in the small subset of patients with follow-up MRI (median, 64% vs 56%). None of the patients without LGE on MR images experienced major adverse cardiovascular events or nonsustained ventricular tachycardia.

These findings suggest that biventricular and left-dominant abnormalities are common in patients with *TMEM43* variants, similar to patients with variants in desmosomal genes such as *DSP* (17). Male patients had higher prevalence of right ventricular dilatation compared with female patients (80% vs 11%), suggesting that there may be sex-related differences in phenotypic expression (5,18). Cardiac MRI findings were progressive with new abnormalities and worsening left ventricular systolic function in the small subset of patients who underwent follow-up MRI. This observation suggests the need for ongoing clinical and imaging follow-up even among patients with initial normal MRI findings (19).

LGE was frequent, involving the left ventricle in 78% of patients and right ventricle in 44% of patients, with a ringlike pattern in 44% of patients. The prevalence of ringlike LGE in

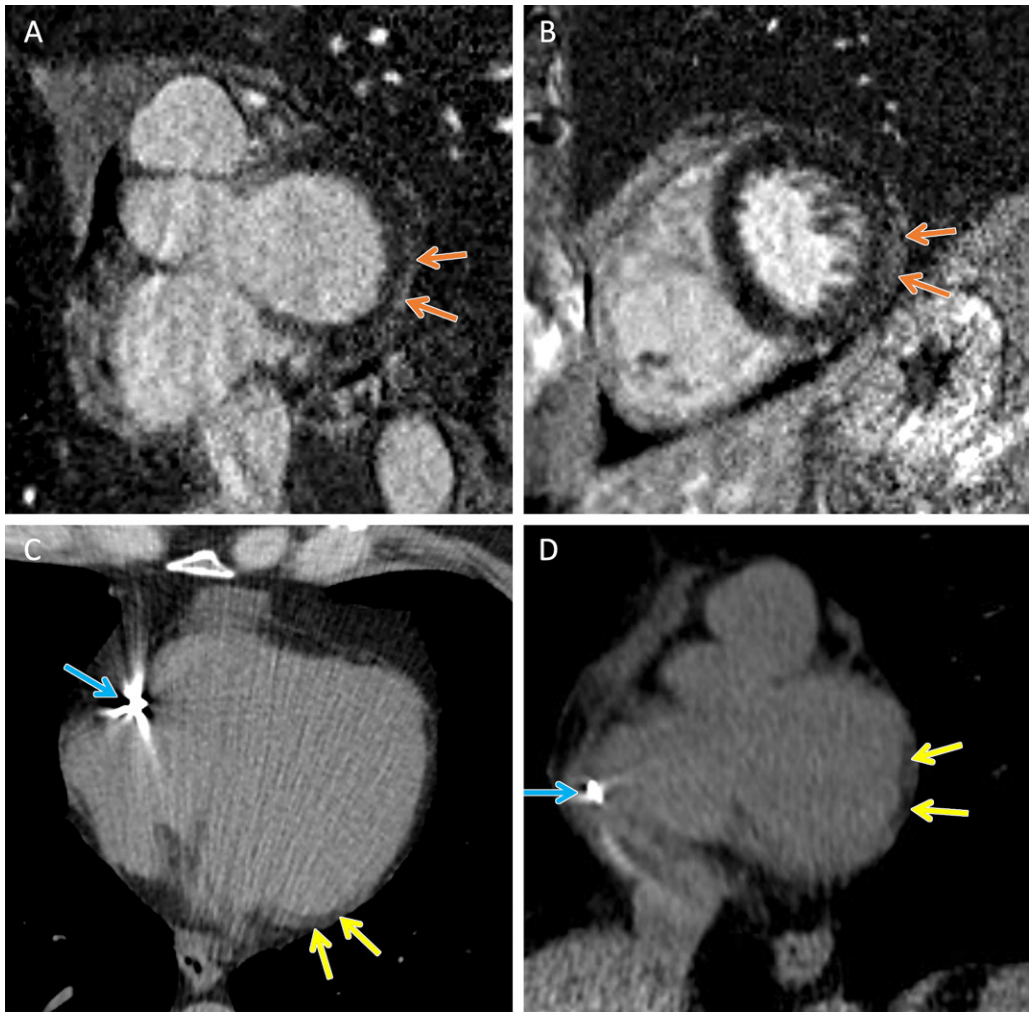

Figure 2: *TMEM43* arrhythmogenic cardiomyopathy. Cardiac CT and MR images in a female patient between 50 and 59 years of age (exact age not provided due to potential reidentification risk) with a *TMEM43* variant of unknown significance (p.Glu142Gly) with premature ventricular beats at Holter monitoring. **(A, B)** Short-axis late gadolinium enhancement images at the **(A)** base and **(B)** midventricle demonstrate subepicardial late gadolinium enhancement involving the basal to mid inferolateral wall (orange arrows). **(C)** Axial and **(D)** short-axis noncontrast cardiac CT images demonstrate subepicardial fat along the lateral basal left ventricular wall (yellow arrows) and right ventricular implantable cardioverter defibrillator lead (blue arrows).

this case series is lower than a reported prevalence of 78% in patients with *DSP*-associated cardiomyopathy (20). However, further study is needed to compare MRI findings between different ACM-related genotypes. The predominant pattern of LGE was subepicardial, and the most common segment involved was the basal inferolateral wall. All patients who experienced major adverse cardiovascular events and nonsustained ventricular tachycardia during follow-up had LGE on cardiac MR images, raising the possibility that LGE may be an adverse prognostic indicator in ACM caused by a *TMEM43* variant, as in other cardiomyopathies (21,22). In a prior study of 60 patients with ACM, cardiac MRI findings including LGE and high T1 were associated with heart failure–related event risk (23). In our case series, there were no major adverse cardiovascular events or nonsustained ventricular tachycardia events in patients without LGE during a median of 5.4 years of clinical follow-up. Given the association of LGE with sudden cardiac death and the importance of LGE in the appropriate diagnosis of left-sided ACM variants, cardiac MRI protocols should include LGE imaging in patients with pathogenic *TMEM43* variants (24,25).

In a genome-wide association study of cardiac MRI-derived LV measurements in 36 041 UK Biobank participants, common genetic variants were identified in loci near 12 mendelian cardiomyopathy-linked genes, including *TMEM43* (26). Of note, not all variants identified in genes that cause mendelian disorders are considered pathogenic. Variant guidelines exist to classify variants into categories ranging from pathogenic to benign based on criteria using typical types of variant evidence, including population, computational, functional, and segregation data (10). Patients with *TMEM43* variants classified as likely benign and benign were not included in our case series.

Limitations of this case series include a small sample size and lack of a comparator group. However, to our knowledge, only isolated cases of cardiac MRI findings in *TMEM43*

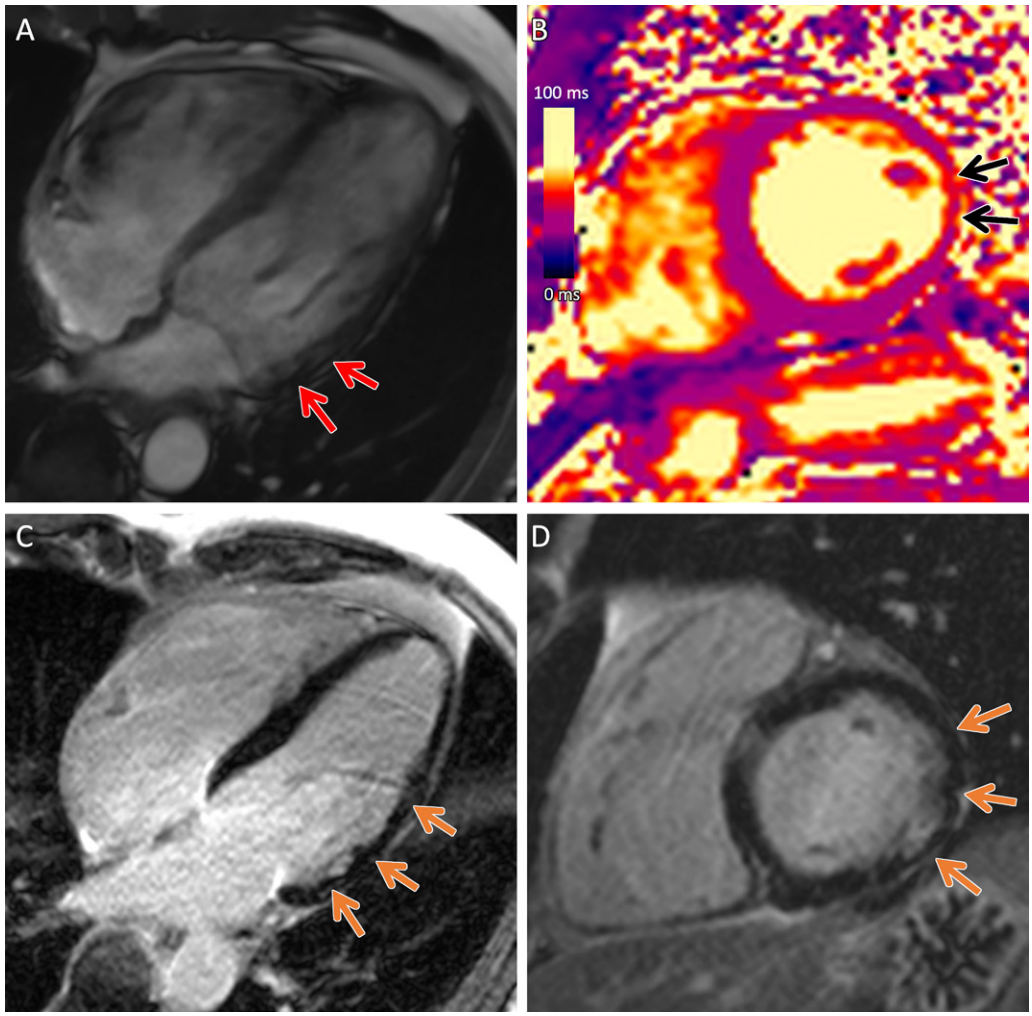

Figure 3: Arrhythmogenic cardiomyopathy with *TMEM43* pathogenic variant (p.Ser358Leu). Cardiac 3-T MR images in a male patient between 50 and 59 years of age (exact age not provided due to potential reidentification risk) with chest pain and premature ventricular beats at Holter monitoring. The patient had a family history of arrhythmogenic cardiomyopathy. **(A)** Four-chamber steady-state free precession MR image demonstrates subepicardial chemical shift artifact along the basal to midventricular lateral left ventricular wall (red arrows). **(B)** Native T2 map demonstrates regional high T2 values at the midventricular inferolateral wall (black arrows). **(C)** Four-chamber and **(D)** short-axis late gadolinium enhancement images demonstrate subepicardial late gadolinium enhancement involving the basal to midventricular anterolateral and inferolateral wall (orange arrows).

variants have been published to date. Importantly, MRI protocols varied and not all included LGE imaging, as many had been performed using shorter noncontrast protocols focused on evaluation of right ventricular size and function. Therefore, the prevalence and extent of left ventricular abnormalities might be underestimated.

In conclusion, variants in the *TMEM43* gene are associated with high prevalence of subepicardial LGE on cardiac MR images with progressive left ventricular dysfunction. Further studies are needed to evaluate the association between cardiac imaging findings and adverse outcomes using standardized protocols and longer-term follow-up.

Author contributions: Guarantor of integrity of entire study, **K.H.**; study concepts/study design or data acquisition or data analysis/interpretation, all authors; manuscript drafting or manuscript revision for important intellectual content, all authors; approval of final version of submitted manuscript, all authors; agrees to ensure any questions related to the work are appropriately resolved, all authors; literature research, **J.M.**, **E.H.**, **D.S.**, **K.H.**; clinical studies, **J.M.**, **E.H.**, **D.S.**, **K.H.**; statistical analysis, **K.H.**; and manuscript editing, all authors

Disclosures of conflicts of interest: J.M. No relevant relationships. **E.H.** No relevant relationships. **M.C.** Speaker honoraria from Blueprint Genetics. **Y.M.** No relevant relationships. **M.H.G.** No relevant relationships. **P.T.** Consultation fees from GE. **D.S.** No relevant relationships. **K.H.** Payment from Sanofi; associate editor for *Radiology* and *Radiology: Cardiothoracic Imaging*.

References

1. Corrado D, Basso C, Judge DP. Arrhythmogenic Cardiomyopathy. Circ Res 2017;121(7):784–802.
2. Marcus FI, Fontaine GH, Guiraudon G, et al. Right ventricular dysplasia: a report of 24 adult cases. Circulation 1982;65(2):384–398.
3. Corrado D, Perazzolo Marra M, Zorzi A, et al. Diagnosis of arrhythmogenic cardiomyopathy: The Padua criteria. Int J Cardiol 2020;319:106–114.
4. Fressart V, Duthoit G, Donal E, et al. Desmosomal gene analysis in arrhythmogenic right ventricular dysplasia/cardiomyopathy: spectrum of mutations and clinical impact in practice. Europace 2010;12(6):861–868.
5. Merner ND, Hodgkinson KA, Haywood AFM, et al. Arrhythmogenic right ventricular cardiomyopathy type 5 is a fully penetrant, lethal arrhythmic disorder caused by a missense mutation in the TMEM43 gene. Am J Hum Genet 2008;82(4):809–821.
6. Milting H, Klauke B, Christensen AH, et al. The TMEM43 Newfoundland mutation p.S358L causing ARVC-5 was imported from Europe and increases the stiffness of the cell nucleus. Eur Heart J 2015;36(14):872–881.

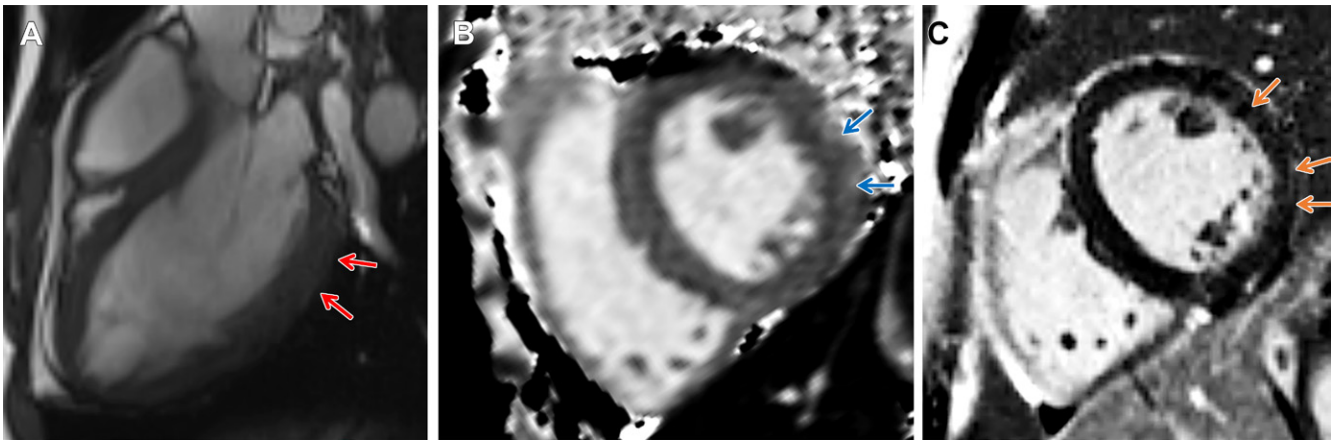

Figure 4: Arrhythmogenic cardiomyopathy with *TMEM43* pathogenic variant (p.Ser358Leu). Short-axis 3-T MR images in a male patient between 18 and 19 years of age (exact age not provided due to potential reidentification risk) with palpitations and premature ventricular beats at Holter monitoring. He had a family history of arrhythmogenic cardiomyopathy in his grandfather, father, and brother. **(A)** Three-chamber steady-state free precession MR image demonstrates subepicardial chemical shift artifact along the basal to mid left ventricular inferolateral wall (red arrows). **(B)** Native T1 map demonstrates regional high T1 values at the subepicardial midventricular inferolateral wall (blue arrows). **(C)** There is subepicardial late gadolinium enhancement involving the midventricular anterior wall, anterolateral wall, and inferolateral wall (orange arrows).

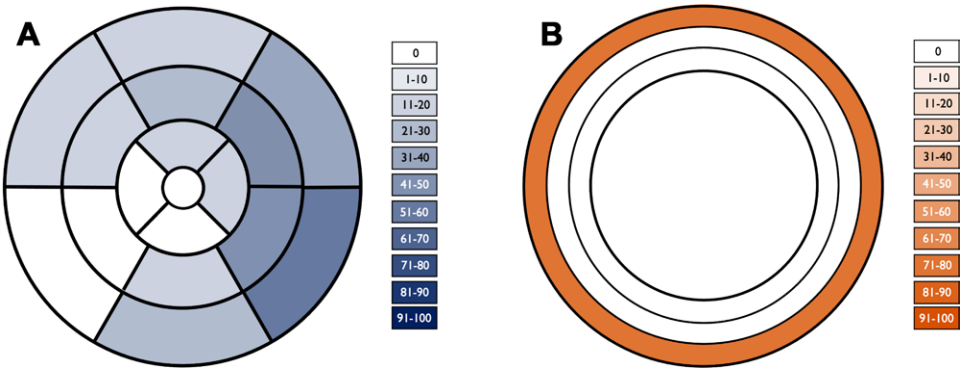

Figure 5: Segmental distribution of late gadolinium enhancement. **(A)** Color-shaded polar plot represents the percentage of patients with late gadolinium enhancement for each myocardial segment according to a standardized 17-segment model. **(B)** Color-shaded plot of the ventricular myocardium represents the percentage of patients with late gadolinium enhancement in each myocardial layer (from outer to inner: subepicardial, midwall, and subendocardial).

7. Baskin B, Skinner JR, Sanatani S, et al. TMEM43 mutations associated with arrhythmogenic right ventricular cardiomyopathy in non-Newfoundland populations. Hum Genet 2013;132(11):1245–1252.
8. Dominguez F, Zorio E, Jimenez-Jaimez J, et al. Clinical characteristics and determinants of the phenotype in TMEM43 arrhythmogenic right ventricular cardiomyopathy type 5. Heart Rhythm 2020;17(6):945–954.
9. Manole S, Pintican R, Popa G, et al. Diagnostic Challenges in Rare Causes of Arrhythmogenic Cardiomyopathy-The Role of Cardiac MRI. J Pers Med 2022;12(2):187.
10. Richards S, Aziz N, Bale S, et al. Standards and guidelines for the interpretation of sequence variants: a joint consensus recommendation of the American College of Medical Genetics and Genomics and the Association for Molecular Pathology. Genet Med 2015;17(5):405–424.
11. Marcus FI, McKenna WJ, Sherrill D, et al. Diagnosis of arrhythmogenic right ventricular cardiomyopathy/dysplasia: proposed modification of the task force criteria. Circulation 2010;121(13):1533–1541.
12. Schulz-Menger J, Bluemke DA, Bremerich J, et al. Standardized image interpretation and post-processing in cardiovascular magnetic resonance - 2020 update : Society for Cardiovascular Magnetic Resonance (SCMR): Board of Trustees Task Force on Standardized Post-Processing. J Cardiovasc Magn Reson 2020;22(1):19.
13. Kawel-Boehm N, Hetzel SJ, Ambale-Venkatesh B, et al. Reference ranges ("normal values") for cardiovascular magnetic resonance (CMR) in adults and children: 2020 update. J Cardiovasc Magn Reson 2020;22(1):87. [Published correction appears in J Cardiovasc Magn Reson 2021;23(1):114.]
14. Cerqueira MD, Weissman NJ, Dilsizian V, et al. Standardized myocardial segmentation and nomenclature for tomographic imaging of the heart. A statement for healthcare professionals from the Cardiac Imaging Committee of the Council on Clinical Cardiology of the American Heart Association. Circulation 2002;105(4):539–542.
15. Graziosi M, Ditaranto R, Rapezzi C, et al. Clinical presentations leading to arrhythmogenic left ventricular cardiomyopathy. Open Heart 2022;9(1):e001914.
16. Warnica W, Al-Arnawoot A, Stanimirovic A, et al. Clinical Impact of Cardiac MRI T1 and T2 Parametric Mapping in Patients with Suspected Cardiomyopathy. Radiology 2022;305(2):319–326.
17. Smith ED, Lakdawala NK, Papoutsidakis N, et al. Desmoplakin Cardiomyopathy, a Fibrotic and Inflammatory Form of Cardiomyopathy Distinct From Typical Dilated or Arrhythmogenic Right Ventricular Cardiomyopathy. Circulation 2020;141(23):1872–1884.
18. Hodgkinson KA, Connors SP, Merner N, et al. The natural history of a genetic subtype of arrhythmogenic right ventricular cardiomyopathy caused by a p.S358L mutation in TMEM43. Clin Genet 2013;83(4):321–331.
19. Roberts WC, Ko JM, Kuiper JJ, Hall SA, Meyer DM. Some previously neglected examples of arrhythmogenic right ventricular dysplasia/cardiomyopathy and frequency of its various reported manifestations. Am J Cardiol 2010;106(2):268–274.
20. Augusto JB, Eiros R, Nakou E, et al. Dilated cardiomyopathy and arrhythmogenic left ventricular cardiomyopathy: a comprehensive genotype-imaging phenotype study. Eur Heart J Cardiovasc Imaging 2020;21(3):326–336.

21. Hanneman K, Karur GR, Wasim S, Wald RM, Iwanochko RM, Morel CF. Left Ventricular Hypertrophy and Late Gadolinium Enhancement at Cardiac MRI Are Associated with Adverse Cardiac Events in Fabry Disease. Radiology 2020;294(1):42–49.
22. Aitken M, Davidson M, Chan MV, et al. Prognostic Value of Cardiac MRI and FDG PET in Cardiac Sarcoidosis: A Systematic Review and Meta-Analysis. Radiology 2023;307(2):e222483.
23. Chun KH, Oh J, Hong YJ, et al. Prognostic Cardiac Magnetic Resonance Markers of Left Ventricular Involvement in Arrhythmogenic Cardiomyopathy for Predicting Heart Failure Outcomes. J Am Heart Assoc 2022;11(6):e023167.
24. Kramer CM, Barkhausen J, Bucciarelli-Ducci C, Flamm SD, Kim RJ, Nagel E. Standardized cardiovascular magnetic resonance imaging (CMR) protocols: 2020 update. J Cardiovasc Magn Reson 2020;22(1):17.
25. Corrado D, Basso C. Arrhythmogenic left ventricular cardiomyopathy. Heart 2022;108(9):733–743.
26. Pirruccello JP, Bick A, Wang M, et al. Analysis of cardiac magnetic resonance imaging in 36,000 individuals yields genetic insights into dilated cardiomyopathy. Nat Commun 2020;11(1):2254.